HHS Public Access

Author manuscript

Nat Immunol. Author manuscript; available in PMC 2010 August 01.

Published in final edited form as:

Nat Immunol. 2010 February ; 11(2): 162–170. doi:10.1038/ni.1830.

CXCR4 acts as a costimulator during thymic β selection

Paul C. Trampont[1], **Annie-Carole Tosello-Trampont**[1], **Yuelei Shen**[2], **Amanda K. Duley**[3], **Timothy P. Bender**[1,3], **Ann E. Sutherland**[4], **Dan R. Littman**[2], and **Kodi S. Ravichandran**[1,3]

[1]Carter Immunology Center, University of Virginia, Charlottesville, VA 22908

[3]Department of Microbiology, University of Virginia, Charlottesville, VA 22908

[4]Department of Cell Biology, University of Virginia, Charlottesville, VA 22908

[2]Howard Hughes Medical Institute, Kimmel Center for Biology and Medicine, Skirball Institute, and New York University School of Medicine, New York, NY1001.

Abstract

Passage through the β-selection developmental checkpoint requires productive rearrangement of *Tcrb* gene segments and formation of a pre-T cell receptor (pre-TCR) on the surface of $CD4^{-}CD8^{-}$ thymocytes. How other receptors influence β-selection is less well understood. Here, we define a new role for the chemokine receptor CXCR4 during T cell development. CXCR4 functionally associates with the pre-TCR and influences β-selection by regulating steady-state localization of immature thymocytes within thymic sub-regions, by facilitating optimal pre-TCR-induced survival signals, and by promoting thymocyte proliferation. We also characterize functionally relevant signaling molecules downstream of CXCR4 and the pre-TCR in thymocytes. These data designate CXCR4 as a co-stimulator of the pre-TCR during β-selection.

INTRODUCTION

The thymic microenvironment supports the differentiation and proliferation of bone marrow-derived progenitors as they enter and migrate through the thymus. Immature thymocytes that lack the expression of the surface molecules CD4 and CD8 (referred to as double negative, DN) can be further subdivided into four distinct developmental stages (DN1, DN2, DN3 and DN4) based on the differential expression of surface markers CD44 and CD251, 2. The developmental progression of DN thymocytes from DN1 to DN4 is influenced by their localization within the thymic architecture as well as signals from surface receptors1, 3. DN1 and DN2 thymocytes begin an outward migration from the

Corresponding Author: Kodi S. Ravichandran Carter Immunology Center Bldg MR4- Rm4072D Box 801386 University of Virginia Charlottesville, VA 22908 ravi@virginia.edu Ph: 434-243-6093 Fax: 434-924-1221.

AUTHOR CONTRIBUTIONS

P.C.T. designed and executed the experiments, and wrote the manuscript. A-C. T-T. performed the experiments for Figure 6a,c,e, and f, as well as Figure 7a and b, and helped with the manuscript. A.K.D. set-up all the required breeding and provided the $Rag2^{-/-}$ and $Rag2^{-/-}TCR\beta^{+}$ mice and provided assistance for Figure 3a. Y.S. provided the data in Figure 1b. T.B.P., A.E.S. provided access to mouse strains and reagents. D.R.L. shared unpublished information, and provided the floxed *Cxcr4* mouse strain and intellectual input. K.S.R. supervised the overall design, conduct and interpretation of the experiments, and the writing of the manuscript.

The authors declare no competing financial interests in publication of this manuscript.

cortico-medullary junction toward the outer cortex, with the DN3 subset localizing mainly at or near the sub-capsular zone (SCZ)4. The β-selection developmental checkpoint, which screens for productive *Tcrb* rearrangement and assembly of a surface pre-T cell receptor (pre-TCR) complex, begins at the DN3 stage and is competed during the DN4 stage. This β-selection process coincides with a movement of the DN4 cells from the cortex back toward the medulla. Thymocytes that successfully progress through this checkpoint begin to express both CD4 and CD8 (referred to as double positive, DP), undergo further maturation and differentiate into cells expressing only CD4 or CD8 (single positive, SP).

Chemokines and their receptors regulate the carefully orchestrated migration patterns of thymocytes, and may provide additional signals that influence thymocyte differentiation5, 6. However, the specific chemokines that function just prior to or during the β-selection checkpoint, and how they might influence pre-TCR signals are not well understood. CXCR4 (http://www.signaling-gateway.org/molecule/query?afcsid=A000636) and its natural ligand SDF-1α (also called CXCL12) are widely expressed in tissues and play a major role in embryonic development7, hematopoiesis8, organogenesis and vascularization9, 10. In addition to regulating trafficking11 and homing of hematopoietic progenitors, CXCR4 acts as a co-receptor for human immunodeficiency virus 1 (HIV-1)12. SDF-1α and CXCR4 have been linked to egress of mature single positive thymocytes from the thymus13, 14. CXCR4 also potentiates responses of peripheral T cells to TCR signals15, 16. However, the role of CXCR4 in regulating the β-selection checkpoint is unknown. An earlier study using a bone marrow chimera approach and Lck-Cre-mediated deletion of CXCR4 reported a developmental block at the DN1 stage17. However, this observation is puzzling as the developmental arrest seen by these authors occurred before the stage at which Lck-Cre-mediated deletion of CXCR4 expression would be predicted to occur. This observation may be due to technical aspects of the bone marrow chimera approach, possibly related to colonizing niches in the thymus or competition between transferred and host progenitors. Thus, the role of CXCR4 in DN thymocyte development, specifically at the β-selection step, and how CXCR4 signals may integrate with pre-TCR signals remain to be defined.

As DN thymocytes undergo β-selection, signals emanating from the pre-TCR and potentially other receptors promote immature thymocyte survival, proliferation and differentiation18. Pre-TCR and Notch receptors expressed on DN thymocytes critically influence proliferation and differentiation during β-selection19. Early DN3 survival can be regulated by the pre-TCR, Notch and interleukin 7 (IL-7) receptor20. Although a function for p53 in rescuing cellularity in CD3γ–deficient thymocytes was initially suggested21, the induction of anti-apoptotic Bcl-2 family proteins and the suppression of pro-apoptotic signals is now thought to influence DN cell survival22 Among the Bcl-2 family members, *Bcl2a1* mRNA expression is upregulated by the pre-TCR during β-selection in a manner dependent on p65 NF-κB, which also has been linked to cell survival signals in early thymic development23, 24. While chemokines may regulate events beyond the localization of thymocytes within the thymic architecture, the role of chemokine receptors in regulating the survival, proliferation and differentiation signals during β-selection remains unclear.

In this report, by disrupting CXCR4 expression during DN2 and DN3 stages, we identified a key role for CXCR4 during β-selection. We also defined a functional interplay between

CXCR4 and pre-TCR, designating CXCR4 as a non-redundant costimulator regulating pre-TCR dependent signals in DN thymocytes.

RESULTS

CXCR4 is needed for progression through β-selection

We first assessed the expression of CXCR4 on DN subsets. DN2 and DN3 thymocytes expressed the highest amounts of surface CXCR4, with lower expression detected on DN4 thymocytes (Fig. 1a). CXCR4 protein expression correlated with *Cxcr4* mRNA expression within the DN subsets (Fig. 1b), and was consistent with an earlier report17. We then examined the localization of SDF-1α within the thymus via immunofluorescence. SDF-1α was detected throughout the cortex, including in many microvessels, and was expressed at the thymic subcapsular zone (SCZ) (Supplementary Fig. 1). Staining for CD25 revealed an enrichment of $CD25^+$ cells in the SCZ, which colocalized with the enriched SDF-1α in the SCZ (Supplementary Fig. 1). Although CD25 marks both DN2 and DN3 subsets, $CD25^+$ cells within the SCZ are primarily DN3 thymocytes25. It is noteworthy that CXCR7, the second receptor for SDF-1α, has a different expression pattern than CXCR4 in thymic subsets (Fig. 1b), and genetic deletion of *Cxcr7* results in no defects in hematopoiesis26; moreover, the C57BL/6 mice we use in these studies do not express CXCR726.

We then used pharmacological and genetic approaches to test the biological importance of SDF-1α and CXCR4 during β-selection *in vivo*. First, we injected newborn mice with AMD3100, a CXCR4 antagonist that blocks SDF-1α-induced CXCR4 signaling27 (Supplementary Fig. 2a). In the AMD3100-treated mice, we detected a relative increase in the DN3 population and a decrease in DN4 thymocytes (Fig. 1c). There was also a slight decrease in thymic cellularity, but this was not statistically significant. These data pointed to a possible role for SDF-1α-induced CXCR4 signaling in DN3 to DN4 progression, although it was difficult to resolve primary versus secondary effects of AMD3100 treatment in this experiment.

To genetically assess the role of CXCR4 in DN thymocyte development, we engineered mice with a floxed *Cxcr4* locus ($Cxcr4^{fl/fl}$)28 and crossed them with mice expressing the Cre recombinase under the Lck proximal promoter, which mediates deletion of floxed loci in DN2 and DN3 thymocytes29 (Supplementary fig. 2b). Lck-Cre^+ $Cxcr4^{fl/fl}$ mice contained fewer thymocytes than control *lck*-Cre/$Cxcr4^{fllwt}$ mice (Fig. 1d). There was also a 3-4 fold increase in the percentage of DN thymocytes in the Lck-Cre^+ $Cxcr4^{fl/fl}$ mice, as well as an increase in DN3 thymocytes with a concomitant decrease in DN4 thymocytes (Fig. 1d). The absolute numbers of each thymic subset confirmed the decreased transition from DN3 to DN4 in Lck-Cre^+ $Cxcr4^{fl/fl}$ mice (Fig. 1e). It is noteworthy that γδ thymocyte numbers were unaffected under these conditions (data not shown). These data suggest an essential role for CXCR4 expression on DN3 thymocytes for optimal progression through β-selection.

CXCR4 in thymocyte localization and survival

Differentiation of DN thymocytes occurs in distinct but tightly regulated locations in the cortex4. In wild-type C57BL/6 mice, $CD25^+$ DN3 thymocytes were more abundant in the

subcapsular zone (SCZ) in the outer cortex, compared to the lower cortex and the cortico-medullary junction (CMJ)4 (Supplementary Fig. 1). In contrast, $CD25^+$ thymocytes in the Lck-Cre^+ *Cxcr4*$^{fl/fl}$ thymi appeared to be aberrantly distributed between the SCZ and lower parts of the cortex (Fig. 2a), with significant accumulation in the lower cortex. Quantification of the CD25 signal intensity within the SCZ, cortex, and CMJ indicated that in Lck-Cre^+ *Cxcr4*$^{fl/fl}$ thymi, $CD25^+$ cells resided mostly in the lower parts of the cortex while in control thymi a greater fraction of $CD25^+$ cells were at the SCZ (Fig. 2b). This aberrant distribution was not due to altered SDF-1α expression, since the SDF-1α staining within the thymi of Lck-Cre^+ *Cxcr4*$^{fl/fl}$ mice was comparable to control littermates (Fig. 2a). This observation was consistent with the reduced migration to SDF-1α by DN3 and DN4 cells from *lck*-Cre/*Cxcr4*$^{fl/fl}$ mice (Supplementary Fig. 2c).

Since SDF-1α-induced CXCR4 signaling has been linked to cell survival30, 31 , we asked whether the altered localization of CXCR4-null DN3 thymocytes could have affected their viability and thereby contributed to the decreased thymocyte numbers in Lck-Cre^+ *Cxcr4*$^{fl/fl}$mice. We compared thymic cortical sections from Lck-Cre^+ *Cxcr4*$^{fl/fl}$ mice and control *lck*-Cre/*Cxcr4*$^{wt/wt}$ mice for apoptotic cells by single stranded DNA staining (apostain) (Fig. 2c). We noticed a much greater number of apoptotic nuclei Lck-Cre^+ *Cxcr4*$^{fl/fl}$ mice compared to controls (Fig. 2c). Quantitation of multiple sections from different mice indicated a three-fold increase in the number of apoptotic nuclei in the cortex of *lck*-Cre/*Cxcr4*$^{fl/fl}$ thymi compared to control thymi (Fig. 2d). It is important to note that apoptotic nuclei were not detected in the medulla of the Lck-Cre^+ *Cxcr4*$^{fl/fl}$ mice (Fig. 2c). Furthermore, when mice were injected with dexamethasone many apoptotic nuclei were seen in different parts of the cortex and medulla (Supplementary Fig. 3). Thus, the increased cell death in the Lck-Cre^+ *Cxcr4*$^{fl/fl}$ mice correlated with regions of the cortex where the $CD25^+$ thymocytes appear to accumulate.

Loss of CXCR4 impairs DN3 maturation

We then investigated whether the developmental defect observed *in vivo* is intrinsic to thymocytes lacking CXCR4, and whether the increased apoptosis would also be recapitulated *ex vivo*. We assessed the transition of DN3 thymocytes to DN4 (and subsequently DP) stages on OP9-DL1 stromal cells32. We first confirmed that OP9-DL1 stromal cells express *Sdf1* mRNA and protein (Supplementary Fig. 4a,b).

We added purified ‘early’ DN3 thymocytes (DN3e, small pre-selection $CD4^-CD8^-CD44^-CD25^+$ cells) from control and Lck-Cre^+ *Cxcr4*$^{fl/fl}$ mice to OP9-DL1 cells, and assessed the emergence of DN4 and DP thymocytes in a time course over 8 days (Fig. 3a, Supplementary Fig 5a). As thymocytes underwent developmental progression, we noticed a marked decrease in the absolute number and the relative percentage of DN4 and DP cells among the thymocytes recovered from the Lck-Cre^+ *Cxcr4*$^{fl/fl}$ cultures, essentially recapitulating the phenotype seen in Lck-Cre^+ *Cxcr4*$^{fl/fl}$ mice (Fig. 3b). This result might also occur due to an unexpected effect of CXCR4 on Notch1 expression on the thymocytes; however, the loss of CXCR4 expression did not impair Notch1 expression in the different thymic subsets (Supplementary Fig. 4c).

It was still possible that the defect observed in the OP9-DL1 cultures after seeing DN3e thymocytes could have arisen from a secondary effect, as the DN3e cells were initially mislocalized in the Lck-Cre^{+} *Cxcr4*$^{fl/fl}$ mice. To test this possibility we took three approaches. First, we sorted bone marrow progenitor cells (Sca1+ c-kit+) from Lck-Cre^{+} *Cxcr4*$^{fl/fl}$ mice and control *lck-Cre/Cxcr4*$^{wt/wt}$ mice, seeded them on OP9-DL1 cells and analyzed them over a 22-day period (Fig. 3c). The bone marrow progenitor cells from both the control and the Lck-Cre^{+} *Cxcr4*$^{fl/fl}$ mice showed normal development of Thy1+ cells up to the DN2 stage (on Day16), comparable fractions that begun to mature into DN3 cells, and similar total cell numbers on Day 18 (Fig.3d). However, by day 22 progenitors from Lck-Cre^{+} *Cxcr4*$^{fl/fl}$ mice showed a severe defect in absolute cell numbers and in the DN3 to DN4 transition (Fig. 3d). Since the DN3 thymocytes in these cultures arose from bone marrow progenitor cells *ex vivo*, this suggests that the defect in DN3 to DN4 transition due to lack of CXCR4 is intrinsic to the thymocytes, and not a secondary effect due to mislocalization. In a second approach, we seeded purified DN1 thymocytes from Lck-Cre^{+} *Cxcr4*$^{fl/fl}$ mice and control mice on OP9-DL1 cells. Compared to controls, Lck-Cre^{+} *Cxcr4*$^{fl/fl}$ thymocytes exhibited a strong defect in the DN3 to DN4 transition and in the generation of DP thymocytes, along with decreased absolute cell numbers (Fig. 3e,f). As a third approach, we sorted DN3e thymocytes from control C57BL/6 mice and seeded them on OP9-DL1 cultures in the presence or absence of the CXCR4 antagonist AMD3100. AMD3100 impaired the DN3 to DN4 transition and reduced absolute cell numbers, consistent with the survival defect we observed in DN3 thymocytes from Lck-Cre^{+} *Cxcr4*$^{fl/fl}$ mice (Fig. 3g). Taken together, these data suggested a cell-autonomous requirement for CXCR4 for progression through the β-selection checkpoint, even under conditions of optimal pre-TCR and Notch signaling in the OP9-DL1 system.

CXCR4 is essential for pre-TCR-mediated survival

We next asked how loss of CXCR4 affected apoptosis of DN thymocytes in the *ex vivo* cultures. Sorted DN3e thymocytes were plated on OP9-DL1 cells and cell death was assessed via annexin V staining. There was a progressive increase in the fraction of annexin-V^{+} DN3 thymocytes from Lck-Cre^{+} *Cxcr4*$^{fl/fl}$ mice over time, up to 30% (Fig. 4a,b); under the same conditions the fraction of annexin-V^{+} DN3 thymocytes from control mice remained constant. This suggested that even under conditions of optimal pre-TCR and Notch signaling, CXCR4 is required for DN thymocyte survival.

Pre-TCR signaling induces survival of DN thymocytes during β-selection33. Bcl2A1 (also named Bfl1) is a pre-TCR inducible pro-survival molecule that can protect early thymocytes from cell death24. As survival signals in DN thymocytes appeared defective in the absence of CXCR4, we took two different approaches to ask whether CXCR4 contributes to pre-TCR dependent *Bcl2a1* expression. First, we examined *Bcl2a1* mRNA expression in freshly isolated thymocytes from Lck-Cre^{+} *Cxcr4*$^{fl/fl}$ mice, specifically in the sorted DN3e (pre-selection), DN3L (post-selection), and DN4 populations (Fig. 4c). Bcl2-A1 was upregulated as thymocytes progressed from DN3e to DN4 in control but not Lck-Cre^{+} *Cxcr4*$^{fl/fl}$ mice. In contrast, no significant difference in amounts of *Bcl2l1*, *Bcl2* and *Mcl1* mRNA was observed (data not shown).

As a second independent approach, we asked whether induction of *Bcl2a1* mRNA expression induced by pre-TCR stimulation via intraperitoneal anti-CD3 injection in mice requires CXCR4. In control experiments using *Rag2*$^{-/-}$ mice we established that *Bcl2a1* mRNA expression was induced in DN thymocytes after anti-CD3 injection (Supplemental Fig. S6); it is noteworthy that under these conditions, expression of *Bcl2l1* and *Bcl2* mRNA was not induced, and the expression of *Il2ra* mRNA was decreased as the DN3 thymocytes transitioned to DN4. Interestingly, in Lck-Cre^{+} *Cxcr4*$^{fl/fl}$ mice, Bcl2A1 induction after anti-CD3ε antibody injection was impaired (Fig. 4d). These studies suggest a requirement for CXCR4 in pre-TCR dependent induction of Bcl2A1, which correlates with the survival defect of DN thymocytes in Lck-Cre^{+} *Cxcr4*$^{fl/fl}$ mice.

CXCR4 functions as a co-stimulator with the pre-TCR

The above data also suggested that CXCR4 works together with pre-TCR, perhaps as a costimulator to regulate downstream signaling events during β-selection. To test this hypothesis, we addressed whether the block in DN to DP differentiation due to the loss of CXCR4 could be compensated by sustained TCR signaling. We crossed D011.10 TCR transgenic mice with Lck-Cre^{+} *Cxcr4*$^{fl/fl}$ mice and analyzed the appropriate progeny (Fig. 5a). Interestingly, the expression of the transgenic TCR failed to rescue the defect due to CXCR4, as evidence by the decrease in total thymic cellularity and in DN4 thymocytes in the DO11.10 Lck-Cre^{+} *Cxcr4*$^{fl/fl}$mice (Fig. 5b). We confirmed that the transgenic TCR was indeed expressed in Lck-Cre^{+} *Cxcr4*$^{fl/fl}$ mice (Fig. 5c).

We also took another approach to ask whether a strong signal via crosslinking of the pre-TCR on DN thymocytes, induced by intraperitoneal injection of anti-CD3ε, could rescue the developmental defect in Lck-Cre^{+} *Cxcr4*$^{fl/fl}$ mice (Fig. 5d). While anti-CD3 antibody caused a decreased in total cellularity in both control mice and Lck-Cre^{+} *Cxcr4*$^{fl/fl}$ mice (ascribed to loss of DP thymocytes), the CXCR4-deficient DN3 thymocytes still displayed a block in their progression from DN3 to DN4. This again suggested that CXCR4 provides a non-redundant signal that cannot be overcome by enhanced pre-TCR signaling at the DN3 stage.

A possible function for SDF-1α-induced CXCR4 signaling in promoting cell growth has been ascribed in other tissues34. Therefore, we asked whether there might be a defect in proliferation of CXCR4-deficient thymocytes. Intraperitoneal BrdU injection did not reveal an obvious proliferative defect in CXCR4-deficient thymocytes *in vivo* (data not shown). To test the effect of CXCR4 on proliferation of DN thymocytes *ex vivo*, we seeded CFSE labeled sorted DN3e thymocytes on OP9-DL1 cells. DN thymocytes from control mice proliferated robustly under these conditions, as shown by the dilution of the CSFE signal. In contrast, those DN cells from Lck-Cre^{+} *Cxcr4*$^{fl/fl}$ mice that did survive displayed impaired proliferation (Fig. 5e). This suggests that CXCR4 promotes proliferation as well as survival of DN thymocytes as they undergo β-selection.

Regulation of CXCR4 signaling by the pre-TCR

We next asked whether CXCR4-mediated signals would be influenced by the pre-TCR. Using SDF-1α-mediated chemotaxis as the readout, we tested whether pre-TCR expression influenced CXCR4 dependent thymocyte migration. DN3 thymocytes from *Rag2*$^{-/-}$ mice

(which lack the pre-TCR)35 migrated poorly toward SDF-1α; in contrast, thymocytes from *Rag2*$^{-/-}$ TCRβ transgenic mice36 displayed substantial chemotaxis to SDF-1α (Fig. 6a). It is important to note that thymocytes from *Rag2*$^{-/-}$ and *Rag2*$^{-/-}$ TCRβ transgenic mice displayed similar CXCR4 surface expression (Fig. 6c). Moreover, DN3 thymocytes from *Rag2*$^{-/-}$ TCRβ transgenic mice displayed little migration toward bovine serum albumin, ruling out increased random movement as an explanation for the defective chemotaxis (Fig. 6a).

The above observation indicating a requirement for pre-TCR in regulating CXCR4 dependent events could also be recapitulated in a pair of pre-T cell lines37. The parental SCIET27 line, which lacks the pre-TCR, migrated poorly to SDF-1α, while the pre-TCR expressing derivative SCB29 migrated robustly (Fig. 6b). The two lines had comparable CXCR4 surface expression (Fig. 6c), and the enhanced migration of SCB29 was observed over a range of SDF-1α concentrations (data not shown). As cell migration depends on the ability to rearrange the actin cytoskeleton, we assessed the state of actin polymerization in the two cell lines. SCIET27 cells showed decreased actin polymerization induced by SDF-1α compared to SCB29 cells (Fig. 6d). Lastly, we detected an inducible colocalization between CXCR4 and the pre-TCR as early as 2-5 minutes after SDF-1α stimulation, and this colocalization lasted for 30-60 minutes (Fig. 6e and data not shown). Taken together, these observations suggest a bidirectional crosstalk between CXCR4 and the pre-TCR.

CXCR4 signals involved in DN thymocyte chemotaxis

Our studies implicated Bcl2A1 in CXCR4 and pre-TCR-induced survival. We next sought to identify the signaling intermediates that may be important for CXCR4 and pre-TCR dependent migration of DN thymocytes. Modulating the phosphorylation and activation of Erk kinases (Erk1 and Erk2, collectively referred to here as Erk) has been proposed to be part of the co-stimulatory signal delivered through chemokine receptors38. Thus, we tested SDF-1α and CXCR4 mediated activation of Erk in cells with or without pre-TCR expression. Phosphorylation of Erk induced by SDF-1α in the SCB29 cells was of greater magnitude and sustained duration compared to the pre-TCR negative SCIET27 cells (Fig. 6f). In comparison, we did not detect such a difference in phosphorylation of Akt, another signaling molecule downstream of SDF-1α39 (Supplementary Fig 7). Erk phosphorylation induced by SDF-1α was also seen in primary thymocytes (Supplementary Fig. 8a). We then tested whether inhibition of Erk activation using a membrane-permeable inhibitory Erk1 peptide (iErk peptide)40 in DN3 thymocytes would affect migration to SDF-1α. The migration of DN3 thymocytes to SDF-1α was abrogated by the iErk peptide, but not by a control peptide (Fig. 6g, Supplementary Fig. 9a), consistent with a previous report linking Erk activation to SDF-1α-dependent migration in other tissues41. The iErk peptide inhibited actin polymerization in DN thymocytes in response to SDF-1α (Fig. 6h). This inhibition was not due to negative effects of iErk peptide on the viability of the thymocytes (Supplementary Fig. 8b). These data identify Erk activation as an important signaling event downstream of pre-TCR and CXCR4 that regulates DN3 chemotaxis to SDF-1α.

Studies in Jurkat cells have suggested that signaling molecules such as ZAP-70 and SLP-76 can affect CXCR4 dependent-calcium responses 22, [59]. We addressed the importance of

calcium flux and Erk activation in migration to SDF-1α. Addition of SDF-1α induced calcium flux in thymocytes in a manner dependent on coexpression of the pre-TCR (Fig. 6i). However, addition of EGTA or BAPTA (which largely blocks the SDF-1α-induced calcium flux) had no significant effect on migration of thymocytes to SDF-1α (Fig. 6g). Similar results were obtained in the pre-TCR expressing SCB29 cell line (Supplementary Fig. 9b). In these same experiments, addition of the iErk peptide strongly blocked the SDF-1α-induced migration. Moreover, the actin polymerization observed after stimulation with SDF-1α was not blocked by addition of BAPTA or EGTA but was inhibited by the iErk peptide. (Fig. 6h,j). Activation of Erk downstream of CXCR4 also appeared to be independent of calcium flux (Supplementary Fig. 9c). Taken together, these data suggest that SDF-1α stimulation in DN thymocytes induces at least two distinguishable downstream signaling events: calcium flux and Erk activation; of these, only Erk activation was critical for migration to SDF-1α.

The adapter protein ShcA (http://www.signaling-gateway.org/molecule/query?afcsid=A002150) becomes tyrosine phosphorylated downstream of the pre-TCR, and ShcA mediated signaling contributes up to 70% of Erk phosphorylation in DN thymocytes42. Moreover, mice with a conditional deletion of ShcA in thymocytes (Lck-Cre^{+} *Shc1*$^{fl/fl}$ mice)42, 43, or mice conditionally expressing a dominant negative mutant ShcA protein (Lck-Cre^{+} ShcFFF)42, 43 display a strong block in DN3 to DN4 progression during β-selection; this block in development correlates with the large reduction in Erk phosphorylation in DN3 and DN4 thymocytes in these mice42, 43. Several observations suggested a role of ShcA downstream of CXCR4 and the pre-TCR. ShcA was phosphorylated after SDF-1α stimulation, and the sustained phosphorylation of ShcA was dependent on the expression of both CXCR4 and the pre-TCR (Fig. 7a). These findings correlate with a recent study describing CXCR4 dependent Shc phosphorylation in Jurkat T cells44. In addition, DN3 thymocytes from Lck-Cre^{+} *Shc1*$^{fl/fl}$ mice (Fig. 7b) and Lck-Cre/ShcFFF mice (data not shown) displayed poor migration to SDF-1α, despite CXCR4 expression comparable to control mice. Reduced migration of thymocytes from Lck-Cre^{+} *Shc1*$^{fl/fl}$ mice was seen at different concentrations of SDF-1α, and there was no apparent defect in migration of these thymocytes to CCL25 (ligand for CCR9) (data not shown). F-Actin polymerization in response to SDF-1α in DN thymocytes from *lck*-Cre/*shc*$^{fl/fl}$ mice was severely impaired (Fig. 7c), although thymocytes from Lck-Cre^{+} *Shc1*$^{fl/fl}$ mice had no apparent defect in calcium flux induced by SDF-1 (Fig. 7d). These findings suggest that ShcA activation and calcium flux represent distinct signaling events induced downstream of CXCR4 stimulation. Interestingly, DN4 thymocytes from Lck-Cre^{+} *Shc1*$^{fl/fl}$ mice retained higher CXCR4 expression on their surface than control thymocytes (Fig. 7e), suggesting a role for ShcA mediated signaling in down-modulation of CXCR4 as cells progress through β-selection. Lastly, the steady state localization and distribution of the CD25^{+} thymocytes was altered in the *lck*-Cre/*Shc*$^{fl/f}$ Lck-Cre^{+} *Shc1*$^{fl/fl}$ mice, with an accumulation in the lower cortex, despite comparable distribution of SDF-1α in the thymic cortex (Fig. 7f,g). Taken together, these data suggested that the adapter protein ShcA and Erk function as relevant early signaling molecules downstream of CXCR4 and the pre-TCR in DN thymocytes.

DISCUSSION

While the requirement for the pre-TCR during β selection has been well established45, how it functions with other receptors expressed on thymocytes has not been well understood. In this report, we identify a previously unrecognized role for the chemokine receptor CXCR4 as a costimulator that functions together with the pre-TCR to promote the DN3 to DN4 transition.

To date, only one study directly addressed the role of CXCR4 in early thymocyte development. Using a bone marrow chimera approach, Plotkin *et al*. reported a role for CXCR4 in regulating thymocyte differentiation at the DN1 and DN2 stages; due to this early arrest, subsequent developmental points were not studied17. However, this observation is puzzling, as this strain of Lck-Cre used by these authors (originally generated by J. Marth) is supposed to initiate deletion of floxed genes only at the late DN stages. The lack of knowledge as to the stage at which Cre-mediated deletion occurred in these mice makes these experiments difficult to interpret. It is noteworthy that re-analysis of thymi from same Lck-Cre^{+} *Cxcr4*$^{fl/fl}$ mice (without bone marrow transplantation) revealed no defect at DN1 and DN2 stages (Chen and Littman, unpublished observations). Thus, the unusual observation by Plotkin *et al*. was likely due to technical aspects of the bone marrow chimera approach, possibly related to colonizing niches in the thymus or competition between transferred and host progenitors.

Based on the studies reported here, we propose that the requirement for CXCR4 in early thymocyte development may involve at least three possible mechanisms. First, CXCR4 appears to regulate the steady-state localization of CD25^{+} thymocytes at the thymic SCZ versus lower parts of the cortex. Second, CXCR4 appears to function as a costimulator with the pre-TCR to provide survival signals that are essential during thymocyte maturation. Third, CXCR4 also promoted optimal proliferation of DN thymocytes.

Our studies also show that the pre-TCR regulates CXCR4-dependent migration, and reciprocally CXCR4 influences pre-TCR dependent induction of survival proteins. Specifically, CXCR4 regulates the ability of the pre-TCR to induce upregulation of Bcl2A1 expression. It is noteworthy that under these conditions, expression of other anti-apoptotic and pro-apoptotic Bcl2 members were not affected by the loss of *Cxcr4*, and that stimulation of CXCR4 alone via addition of SDF-1α did not stimulate upregulation of *Bcl2a1* mRNA in DN thymocytes. Thus, our data suggest that the Bcl2A1 expression in DN thymocytes undergoing β-selection depends on the integration of signals from the pre-TCR and CXCR4. It is possible that posttranslational mechanisms (such as phosphorylation or changes in localization) may also contribute to the balance of pro-apoptotic and anti-apoptotic signals. However, previous studies in Jurkat T cells and mature T cells looking at signaling events downstream of CXCR4 have suggested a role for ZAP-70 and SLP-76 in regulating transcriptional events15, 46. Whether these proteins influence *Bcl2a1* mRNA expression downstream of pre-TCR and CXCR4 signals remains to be determined. Autophagy has also been implicated in T lymphocyte survival and a recent study suggested a role for CXCR4 in HIV-induced CD4 cell death through autophagy47. However, in our initial studies, we did

not detect a defect in the transcription of autophagy-related genes in the DN thymic subsets from Lck-Cre^{+} *Cxcr4*$^{fl/fl}$ mice.

With respect to CXCR4 and SDF-1α induced migration of DN thymocytes, we identify a key role for phosphorylation and activation of Erk and the adapter protein ShcA in actin polymerization. As ShcA and Erk are ubiquitously expressed, these signaling intermediates downstream of CXCR4 could be relevant not only for T cell biologists but also those studying CXCR4-dependent migration of stem cells and neuronal cells.

Lastly, CXCR4 is also a coreceptor for HIV, and the phenotype of disturbed thymic development in pediatric AIDS patients is not well-understood 48. Interestingly, CXCR4 mediated actin rearrangements are critical in establishment of HIV infection in resting T cells 49. Our findings indicating that interference with CXCR4 function affects thymic development, and that Erk and ShcA regulate actin polymerization downstream of CXCR4, may also shed light on AIDS-related T cell pathologies.

Supplementary Material

Refer to Web version on PubMed Central for supplementary material.

ACKNOWLEDGMENTS

We thank J.C. Zuniga-Pflücker for providing the OP9-DL1 cells, I. Aifantis for the SCIET27 and SCB29 cells, and the flow cytometry and histology core facilities at the University of Virginia for technical assistance. We also thank members of the Ravichandran laboratory, and specifically Ignacio J. Juncadella and M. R. Elliott for technical assistance. We thank J. Lysiak and R. Woodson for help with the Apostain technique. This work was supported by grants from the NIGMS (K.S.R.), NCI (T.P.B.), and the Howard Hughes Medical Institute (D.R.L.).

METHODS

Mice

C57BL/6 and Rag-2-deficient mice were purchased from Taconic. *Cxcr4*$^{fl/fl}$28, *Shc1*$^{fl/fl}$ and the lox-STOP-lox ShcFFF transgenic mice have been described previously42. Mice were bred and maintained under specific pathogen-free conditions at the University of Virginia animal facility according to protocols approved by the Animal Care and Use Committee. Before AMD3100 injection, C57BL/6 newborn mice were weighed to keep the concentration of AMD3100 administered at 5mg/kg50.

Flow cytometry

Thymocytes from 4-6 week-old mice were stained as described previously43. CXCR4 (2B11) antibody was purchased from e-biosciences. Flow cytometry was performed with FACS Canto and the samples analyzed by FlowJo software.

Quantitative PCR

Thymocyte subsets from *Cxcr4*$^{fl/fl}$, Lck-Cre^{+} *Cxcr4*$^{+/+}$ or, Lck-Cre^{+} *Cxcr4*$^{fl/fl}$ mice were electronically sorted based on CD3, CD4, CD8, c-kit, CD44, and CD25 surface expression

after gating out cells expressing hematopoietic lineage markers (CD11b, CD11c, B220, Ly6G, Ter119). Total RNA was then extracted using the Qiagen Qiashredder and RNeasy kit. Reverse transcription was performed using the SuperScript III kit (Invitrogen). Quantitative PCR was carried out using the TaqMan Gene Expression Assays (Applied Biosystems) listed in Supplementary Table 1. Each sample was amplified in duplicate and target transcripts were normalized to *Gapdh* mRNA as an internal control. The relative expression of each target gene was calculated by the "comparative CT method" using StepOne v2.1 software (Applied Biosystems). Quantitative PCR (qPCR) were run on a STEP One Plus instrument (ABI). Standard deviations were calculated after normalization from multiple experiments

Cell lines and OP9-DL1 stromal cell cultures

SCIET27 and SCB29 cell lines were kindly provided by I. Aifantis and cultured as described 37. OP9 stromal cells expressing the Notch ligand delta-like-1 (OP9-DL1) were maintained as described32. DN1 ($CD4^-CD8^-CD3^-CD25^-CD44^+$c-$kit^+$) or DN3 ($CD4^-CD8^-$c-$kit^-CD25^+$) thymocytes from *Cxcr4*$^{fl/fl}$ and Lck-Cre^+ *Cxcr4*$^{fl/fl}$ mice were sorted and plated at 2×10^3 and 10^4 thymocytes per well, respectively, on a layer of non-confluent OP9-DL-1. Co-cultures were grown as described32. To determine the effect of inhibiting Erk kinases or blocking CXCR4 signaling, on DN3 proliferation and differentiation, cells were grown with 50μM of the Erk activation inhibitory peptide I (iErk) (EMD, Calbiochem) or with 1μg/ml AMD3100 (added at the initiation of the cultures and again on day 4). Thymocytes were collected on multiple days and surface expression of Thy1.2, CXCR4, CD4, CD8, CD44 and CD25 was analyzed by flow cytometry. Thymocytes were counted by including reference beads during flow cytometry (Spherotec). Any stromal cells carried over were gated out based on their side scatter and GFP expression. Data are from duplicate sets of analysis.

Immunofluorescence analysis

Thymi were embedded in OCT compound (Torrance) and snap frozen in liquid nitrogen. Four micrometer-thick frozen sections were fixed in acetone for 15 min, air-dried for 30 min and re-hydrated in PBS. Tissue sections were blocked with 2% normal goat serum for 15 minutes and then stained for 60 minutes at room temperature with mouse anti-SDF-1α (P-159x, Santa-Cruz) and CD25-PE (PC61). After incubation, slides were washed three times in PBS and incubated with appropriate fluorochrome linked secondary antibody. Slides were then mounted with ProLong® Gold antifade reagent (Molecular Probes, Invitrogen) and viewed on a Zeiss axioskop microscope. Pictures were taken using an axiocam MRm digital Camera (Zeiss)

CD25 pixel intensity analysis

CD25-stained thymic sections were divided into three areas: the SCZ, the cortex and the CMJ. The pixel intensities were measured by scanning multiple CD25 serial sections from the same slide, as well multiple slides, using NIH image-J software. The values obtained were then plotted as histograms. Data presented are representative of seven C57BL/6 mice, four Lck-Cre^+ *Cxcr4*$^{fl/fl}$, and *five* Lck-Cre^+ *Shc1*$^{fl/fl}$ mice.

Chemotaxis assay

Freshly isolated thymocytes (10^6 cells) were placed on the top chamber of Transwell plates with 5μm pore-size inserts (Costar). To measure migration of thymocytes, upper and lower sides of the Transwell were first coated with 10μg/ml of BSA or murine laminin (3μg/cm^2). Thymocytes were then loaded into the upper chamber, while six hundred microliters of DMEM 1% BSA, containing 40ng/ml (5nM) of SDF-1α (PeproTech) was added into the lower wells. The chemotaxis chambers were incubated at 37°C for 2 hours. The contents of the lower wells were then collected, and the cells were stained for Thy1.2, CD3ε, CD4, CD8, a panel of hematopoietic lineage markers (Gr-1, Ter119, B220, CD11b), and CD44 and CD25. The number of migrating cells was counted using the Cell titer Glo assay Kit (Promega) and a beads based cytometry assay (Spherotec). For chemotaxis assays using cell lines, 10^6 cells were allowed to transmigrate across 5μm pore Transwell inserts for 90 minutes. To determine the effect of inhibiting CXCR4, Erk kinases or chelation of extracellular calcium, cells were pretreated with 0.5μM of AMD3100, 50μM of iErk or 10mM of the calcium chelators EGTA and BAPTA for 30 minutes at 37°C. Input cells were directly added to the lower chamber to obtain the maximal count (100%) and to estimate the migrating fraction. Transwell assays were performed in duplicate for each condition, with thymocytes from a minimum pool of three mice of the same genotype.

Confocal microscopy

SCB29 cells were incubated with biotin-conjugated CXCR4 mAb (Clone 2B11; e-biosciences) and an excess of pre-TCR mAb (Clone 2F5; BD Pharmingen) for 20 min at 4°C, washed in cold PBS buffer without sodium azide and stimulated at 37°C with SDF-1α for the indicated times. After adding cold PBS containing 3% sodium azide, the cells were stained with Streptavidin-FITC and Alexa-647-conjugated goat anti-mouse (Invitrogen). After two washes, cells were spun on to slides, and slides were mounted with ProLong® Gold antifade (Molecular probes). Slides were viewed on a Zeiss confocal microscope.

Detection of apoptotic nuclei in thymic sections

Thymic tissues from *Cxcr4*$^{fl/fl}$ and *lck*-Cre/*Cxcr4*$^{fl/fl}$ mice were formalin-fixed, and tissue sections prepared with routine histological techniques. Thymic sections were stained for single-stranded DNA (ssDNA) using the Apostain detection kit (Bender MedSystems GmbH). Apoptotic cells were revealed as recommended by the manufacturer.

Flow cytometric analysis of F-actin polymerization

To measure actin reorganization, 10^6 cells were stimulated with 10nM SDF-1α for 5 seconds to 2 minutes. Where indicated, cells were pre-incubated for 30 minutes with peptides, calcium chelators or chemical inhibitors as described for the migration assay. The reaction was stopped by fixing the cells with 2% paraformaldehyde (Electron Microscopy Sciences), for 10 min at room temperature. After 2 washes with PBS, cells were stained with Alexa-647-conjugated phalloidin (Molecular Probes) and antibodies specific for surface

markers for 20 minutes at 4°C. Cells were subsequently washed and acquired as described above.

Intracellular Ca^{2+} measurements

Intracellular Ca^{2+} abundance was measured in primary thymocytes or cell lines cells loaded with indo-1 (1 μg/ml/10^6 cells, 20 min, 37°C), in a Hitachi F-2500 fluorescence spectrophotometer. After recording the background for 30 sec, cells were stimulated by injecting SDF-1α (final concentration, 10nM). Ca^{2+} flux was measured as the fluorescence ratio of bound versus unbound forms of Indo-1.

SDF-1α stimulation, immunoprecipitation and immunoblotting

Cell lines or thymocytes at 10^7 cells per ml were resuspended in cold RPMI 1640 with 1% fetal calf serum (FCS) and allowed to rest for 1 hour on ice. Cells were then centrifuged, resuspended in the same buffer and stimulated at 37°C in a time course from 1min to 2 hours with 20nM SDF-1α or for 10 min with 40 nM PMA. For anti-CD3 cross-linking, 2 μg/ml of anti-CD3ε along with 20 μg/ml of $F(ab')^2$ goat anti-mouse for secondary crosslinking was used for 2 min at 37°C. The stimulations were stopped by addition of 1 ml of ice-cold PBS containing phosphatase and protease inhibitors. After cell lysis, ShcA immunoprecipitation and immunoblotting were conducted as previously described42 Phosphorylated ShcA was detected by anti-phosphotyrosine antibody RC20H (Transduction Lab). Total cell lysates were blotted with anti-phospho-Erk1/2 (tyr204, thr202, Cell Signaling), anti-phospho-Akt (ser473, Cell Signaling) or anti-phospho-Shc (tyr239/240, Santa-Cruz).

SDF-1α ELISA

Enzyme-linked immunosorbent assay (ELISA) was performed on cell culture supernatants from OP9-DL1 grown with or without IL-7 and Flt3-L. Cell culture supernatants were standardized for total protein content, before being submitted to ELISA assay using a mouse monoclonal anti-SDF-1α (P-159x, Santa-Cruz), as the capture antibody and a rabbit polyclonal anti-SDF-1α (e-biosciences) as the detection antibody. The standard curve was set using recombinant murine SDF-1α (Peprotech).

Statistical methods

Results are expressed as the mean ± s.d.. Statistical significance was obtained with a two-sided t-test assuming equal variance (α=0.05). Statistical analysis was calculated with the Microsoft Excel program.

REFERENCES

1. Kruisbeek AM, et al. Branching out to gain control: how the pre-TCR is linked to multiple functions. Immunol Today. 2000; 21:637–644. [PubMed: 11114425]
2. Wiest DL, Berger MA, Carleton M. Control of early thymocyte development by the pre-T cell receptor complex: A receptor without a ligand? Semin Immunol. 1999; 11:251–262. [PubMed: 10441211]

3. von Boehmer H. Unique features of the pre-T-cell receptor alpha-chain: not just a surrogate. Nat Rev Immunol. 2005; 5:571–577. [PubMed: 15999096]
4. Petrie HT, Zuniga-Pflucker JC. Zoned out: functional mapping of stromal signaling microenvironments in the thymus. Annu Rev Immunol. 2007; 25:649–679. [PubMed: 17291187]
5. Hollander G, et al. Cellular and molecular events during early thymus development. Immunol Rev. 2006; 209:28–46. [PubMed: 16448532]
6. Takahama Y. Journey through the thymus: stromal guides for T-cell development and selection. Nat Rev Immunol. 2006; 6:127–135. [PubMed: 16491137]
7. Zou YR, Kottmann AH, Kuroda M, Taniuchi I, Littman DR. Function of the chemokine receptor CXCR4 in haematopoiesis and in cerebellar development. Nature. 1998; 393:595–599. [PubMed: 9634238]
8. Nagasawa T, et al. Defects of B-cell lymphopoiesis and bone-marrow myelopoiesis in mice lacking the CXC chemokine PBSF/SDF-1. Nature. 1996; 382:635–638. [PubMed: 8757135]
9. Tachibana K, et al. The chemokine receptor CXCR4 is essential for vascularization of the gastrointestinal tract. Nature. 1998; 393:591–594. [PubMed: 9634237]
10. Ceradini DJ, et al. Progenitor cell trafficking is regulated by hypoxic gradients through HIF-1 induction of SDF-1. Nat Med. 2004; 10:858–864. [PubMed: 15235597]
11. Okada T, et al. Chemokine requirements for B cell entry to lymph nodes and Peyer's patches. J Exp Med. 2002; 196:65–75. [PubMed: 12093871]
12. Feng Y, Broder CC, Kennedy PE, Berger EA. HIV-1 entry cofactor: functional cDNA cloning of a seven-transmembrane, G protein-coupled receptor. Science. 1996; 272:872–877. [PubMed: 8629022]
13. Poznansky MC, et al. Active movement of T cells away from a chemokine. Nat Med. 2000; 6:543–548. [PubMed: 10802710]
14. Cyster JG. Chemorepulsion and thymocyte emigration. J Clin Invest. 2002; 109:1011–1012. [PubMed: 11956237]
15. Kumar A, et al. CXCR4 physically associates with the T cell receptor to signal in T cells. Immunity. 2006; 25:213–224. [PubMed: 16919488]
16. Molon B, et al. T cell costimulation by chemokine receptors. Nat Immunol. 2005; 6:465–471. [PubMed: 15821738]
17. Plotkin J, Prockop SE, Lepique A, Petrie HT. Critical role for CXCR4 signaling in progenitor localization and T cell differentiation in the postnatal thymus. J Immunol. 2003; 171:4521–4527. [PubMed: 14568925]
18. Aifantis I, Mandal M, Sawai K, Ferrando A, Vilimas T. Regulation of T-cell progenitor survival and cell-cycle entry by the pre-T-cell receptor. Immunol Rev. 2006; 209:159–169. [PubMed: 16448541]
19. Ciofani M, Zuniga-Pflucker JC. The thymus as an inductive site for T lymphopoiesis. Annu Rev Cell Dev Biol. 2007; 23:463–493. [PubMed: 17506693]
20. Ciofani M, et al. Obligatory role for cooperative signaling by pre-TCR and Notch during thymocyte differentiation. J Immunol. 2004; 172:5230–5239. [PubMed: 15100261]
21. Haks MC, Krimpenfort P, van den Brakel JH, Kruisbeek AM. Pre-TCR signaling and inactivation of p53 induces crucial cell survival pathways in pre-T cells. Immunity. 1999; 11:91–101. [PubMed: 10435582]
22. Opferman JT, Korsmeyer SJ. Apoptosis in the development and maintenance of the immune system. Nat Immunol. 2003; 4:410–415. [PubMed: 12719730]
23. Voll RE, et al. NF-kappa B activation by the pre-T cell receptor serves as a selective survival signal in T lymphocyte development. Immunity. 2000; 13:677–689. [PubMed: 11114380]
24. Mandal M, et al. The BCL2A1 gene as a pre-T cell receptor-induced regulator of thymocyte survival. J Exp Med. 2005; 201:603–614. [PubMed: 15728238]
25. Lind EF, Prockop SE, Porritt HE, Petrie HT. Mapping precursor movement through the postnatal thymus reveals specific microenvironments supporting defined stages of early lymphoid development. J Exp Med. 2001; 194:127–134. [PubMed: 11457887]

26. Sierro F, et al. Disrupted cardiac development but normal hematopoiesis in mice deficient in the second CXCL12/SDF-1 receptor, CXCR7. Proc Natl Acad Sci U S A. 2007; 104:14759–14764. [PubMed: 17804806]
27. Schols D, et al. Inhibition of T-tropic HIV strains by selective antagonization of the chemokine receptor CXCR4. J Exp Med. 1997; 186:1383–1388. [PubMed: 9334378]
28. Nie Y, et al. The role of CXCR4 in maintaining peripheral B cell compartments and humoral immunity. J Exp Med. 2004; 200:1145–1156. [PubMed: 15520246]
29. Lee PP, et al. A critical role for Dnmt1 and DNA methylation in T cell development, function, and survival. Immunity. 2001; 15:763–774. [PubMed: 11728338]
30. Kabashima K, et al. CXCR4 engagement promotes dendritic cell survival and maturation. Biochem Biophys Res Commun. 2007; 361:1012–1016. [PubMed: 17679142]
31. Suzuki Y, Rahman M, Mitsuya H. Diverse transcriptional response of CD4(+) T cells to stromal cell-derived factor (SDF)-1: cell survival promotion and priming effects of SDF-1 on CD4(+) T cells. J Immunol. 2001; 167:3064–3073. [PubMed: 11544290]
32. Schmitt TM, Zuniga-Pflucker JC. Induction of T cell development from hematopoietic progenitor cells by delta-like-1 in vitro. Immunity. 2002; 17:749–756. [PubMed: 12479821]
33. Ciofani M, Zuniga-Pflucker JC. A survival guide to early T cell development. Immunol Res. 2006; 34:117–132. [PubMed: 16760572]
34. Yang L, et al. Blocking CXCR4-mediated cyclic AMP suppression inhibits brain tumor growth in vivo. Cancer Res. 2007; 67:651–658. [PubMed: 17234775]
35. Shinkai Y, et al. RAG-2-deficient mice lack mature lymphocytes owing to inability to initiate V(D)J rearrangement. Cell. 1992; 68:855–867. [PubMed: 1547487]
36. Shinkai Y, et al. Restoration of T cell development in RAG-2-deficient mice by functional TCR transgenes. Science. 1993; 259:822–825. [PubMed: 8430336]
37. Aifantis I, Gounari F, Scorrano L, Borowski C, von Boehmer H. Constitutive pre-TCR signaling promotes differentiation through Ca2+ mobilization and activation of NF-kappaB and NFAT. Nat Immunol. 2001; 2:403–409. [PubMed: 11323693]
38. Trautmann A. Chemokines as immunotransmitters? Nat Immunol. 2005; 6:427–428. [PubMed: 15843794]
39. Sotsios Y, Whittaker GC, Westwick J, Ward SG. The CXC chemokine stromal cell-derived factor activates a Gi-coupled phosphoinositide 3-kinase in T lymphocytes. J Immunol. 1999; 163:5954–5963. [PubMed: 10570282]
40. Kelemen BR, Hsiao K, Goueli SA. Selective in vivo inhibition of mitogen-activated protein kinase activation using cell-permeable peptides. J Biol Chem. 2002; 277:8741–8748. [PubMed: 11756441]
41. Alsayed Y, et al. Mechanisms of regulation of CXCR4/SDF-1 (CXCL12)-dependent migration and homing in multiple myeloma. Blood. 2007; 109:2708–2717. [PubMed: 17119115]
42. Trampont P, Zhang L, Ravichandran KS. ShcA mediates the dominant pathway to extracellular signal-regulated kinase activation during early thymic development. Mol Cell Biol. 2006; 26:9035–9044. [PubMed: 16982683]
43. Zhang L, Camerini V, Bender TP, Ravichandran KS. A nonredundant role for the adapter protein Shc in thymic T cell development. Nat Immunol. 2002; 3:749–755. [PubMed: 12101399]
44. Patrussi L, et al. p52Shc is required for CXCR4-dependent signaling and chemotaxis in T cells. Blood. 2007; 110:1730–1738. [PubMed: 17537990]
45. von Boehmer H, et al. Crucial function of the pre-T-cell receptor (TCR) in TCR beta selection, TCR beta allelic exclusion and alpha beta versus gamma delta lineage commitment. Immunol Rev. 1998; 165:111–119. [PubMed: 9850856]
46. Kremer KN, Humphreys TD, Kumar A, Qian NX, Hedin KE. Distinct role of ZAP-70 and Src homology 2 domain-containing leukocyte protein of 76 kDa in the prolonged activation of extracellular signal-regulated protein kinase by the stromal cell-derived factor-1 alpha/CXCL12 chemokine. J Immunol. 2003; 171:360–367. [PubMed: 12817019]
47. Espert L, et al. Autophagy is involved in T cell death after binding of HIV-1 envelope proteins to CXCR4. J Clin Invest. 2006; 116:2161–2172. [PubMed: 16886061]

48. Brooks DG, Kitchen SG, Kitchen CM, Scripture-Adams DD, Zack JA. Generation of HIV latency during thymopoiesis. Nat Med. 2001; 7:459–464. [PubMed: 11283673]

49. Yoder A, et al. HIV envelope-CXCR4 signaling activates cofilin to overcome cortical actin restriction in resting CD4 T cells. Cell. 2008; 134:782–792. [PubMed: 18775311]

50. Broxmeyer HE, et al. Transgenic expression of stromal cell-derived factor-1/CXC chemokine ligand 12 enhances myeloid progenitor cell survival/antiapoptosis in vitro in response to growth factor withdrawal and enhances myelopoiesis in vivo. J Immunol. 2003; 170:421–429. [PubMed: 12496427]

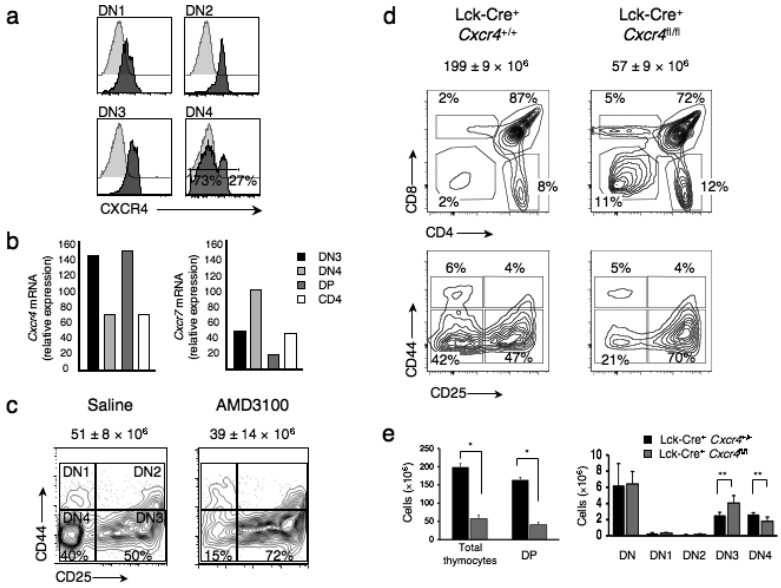

Figure 1.

CXCR4 regulates β-selection *in vivo*. (**a**) CXCR4 surface expression (blue) on DN thymocyte subsets. Grey histograms show staining with isotype-matched control antibody (*n*>5). (**b**) Quantitative PCR analysis of *Cxcr4* and *Cxcr7* expression in DN thymocyte subsets from C57BL/6 mice. Transcript expression was normalized to *Gapdh* within each subset (*n*=2). (**c**) C57BL/6 mice were injected intraperitoneally with saline or the CXCR4 antagonist AMD3100 (every 48 hours for a period of 7 days. A representative flow cytometric profile of DN subsets from one of five mice is shown with the average thymic cellularity indicated above each dot plot (*n*=2). (**d**) Thymi from Lck-Cre^{+} *Cxcr4*$^{+/+}$ and Lck-Cre/*Cxcr4*$^{fl/fl}$ mice were isolated. Total cellularity (above dot plots) and surface marker expression were determined. Lower dot plots are gated on DN thymocytes. *n*>16 for each genotype. (**e**) Absolute numbers of thymic subsets in Lck-Cre^{+} *Cxcr4*$^{+/+}$ and Lck-Cre^{+} *Cxcr4*$^{fl/fl}$ mice. Data show the mean ± s.d. of at least ten littermates for each genotype (4-6 weeks old). Littermates were obtained from 3 or more different breeding cages.

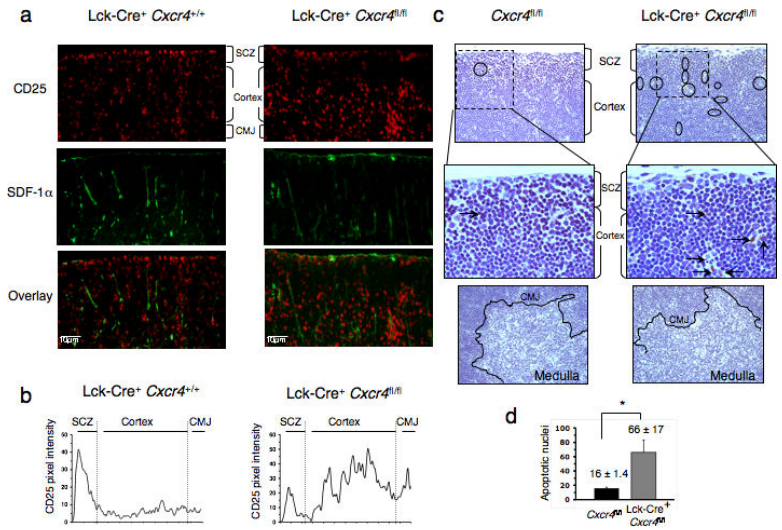

Figure 2.

CXCR4 deletion affects localization and survival of early thymic progenitors *in vivo*. (**a**) Thymic cryosections from Lck-Cre^{+} *Cxcr4*$^{+/+}$ and Lck-Cre^{+} *Cxcr4*$^{fl/fl}$mice (4-6 weeks old) were stained with antibodies to CD25 (red) and SDF-1α (green). (*n*=6). (**b**) The average CD25 pixel intensities within the subcapsular zone (SCZ), cortex and cortico-medullary junction (CMJ) were quantified by scanning multiple serial sections from Lck-Cre^{+} *Cxcr4*$^{+/+}$ and Lck-Cre^{+} *Cxcr4*$^{fl/fl}$mice (three mice per group) (*n*=2). (**c**) Thymic sections from Lck-Cre^{+} *Cxcr4*$^{+/+}$ and Lck-Cre^{+} *Cxcr4*$^{fll/fl}$ mice were stained for fragmented nuclei from apoptotic thymocytes (brown, apostain) and counterstained with hematoxylin (blue background tissue staining). Images show apoptotic nuclei from the SCZ (top and middle panels) and the medulla (bottom panels). *n*=2. Top and bottom panels, original magnification ×20. Middle panel shows boxed region in top panels, original magnification ×40. (*n*=2). (**d**) Apoptotic nuclei in the cortex and at the SCZ were counted from multiple sections and thymi from at least two independent staining out of the same tissues.. Data were plotted as the mean mean ± s.d.

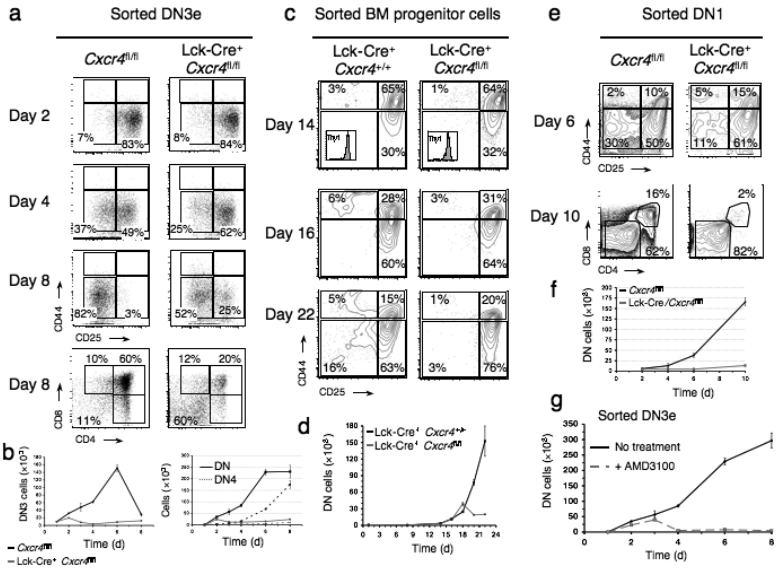

Figure 3.

CXCR4 provides differentiation and survival signals during T cell development. (**a**) Purified DN3e thymocytes from the Lck-Cre^{+} *Cxcr4*$^{fl/fl}$ and Lck-Cre^{+} *Cxcr4*$^{+/+}$ mice (small CD4^{-}CD8^{-}CD3^{-}CD25^{+} thymocytes that were electronically sorted based on their size, after gating out cells expressing any of a panel of hematopoietic lineage markers) were seeded on OP9-DL1 stromal cells. The differentiation to later stages of DN and DP development was determined on days 2, 4 and 8 post-initiation of co-culture. The bottom panels are gated on total thymocytes whereas all other panels are gated on DN cells (*n*=3). (**b**) The absolute numbers of total DN3 thymocytes (left panel) or total DN and DN4 (right panel) in the cultures described in **a** were determined by flow cytometry. Each co-culture was done in triplicates and s.e.m. reflects variation. (**c**) Sca1^{+} c-kit^{+} bone marrow progenitors from indicated mice were electronically sorted based on a panel of hematopoietic lineage markers. Purified hematopoietic progenitors were then seeded on OP9-DL1 stromal cells. Differentiation to later stages of development was determined by flow cytometry on days 14, 16 and 22 post-initiation of co-culture (*n*=2). (**d**) Absolute numbers of cells present in cultures described in **c**. Each co-culture was done in triplicates and s.e.m. reflects variation. (**e**) c-kit^{+} immature thymocytes (DN1) from indicated mice were sorted and seeded on OP9-DL1 cultures and analyzed by flow cytometry on day 3 and 6. Top plots are gated on DN cells and bottom plots are gated on total thymocytes (*n*=2). (**f**) Absolute numbers of cells present in cultures described in **e**. Each co-culture was done in triplicates and s.e.m. reflects variation. (**g**) Purified DN3e cells were seeded on OP9-DL1 cultures in the presence or absence of the CXCR4 antagonist AMD3100, and absolute cell numbers were measured at the indicated time points. Each co-culture was done in triplicates and s.e.m. reflects variation. (*n*>3).

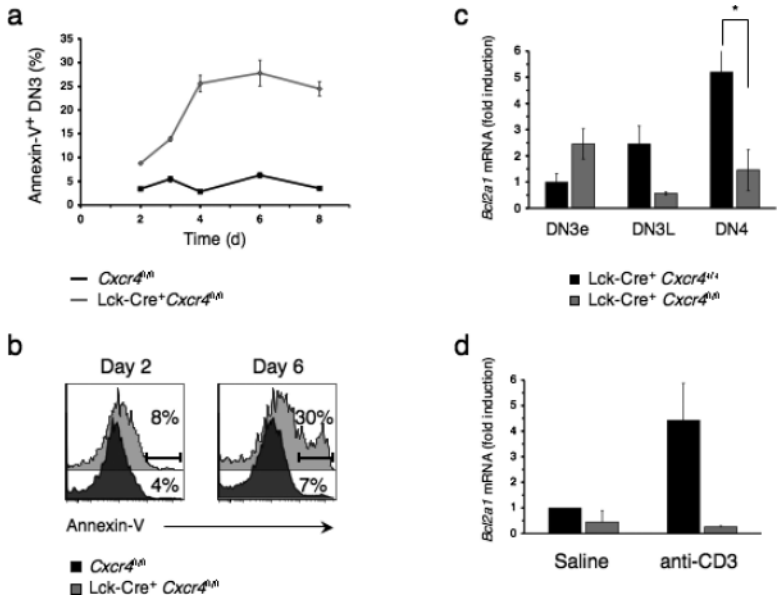

Figure 4.

CXCR4 is required for pre-TCR dependent survival signals. (**a**) Cell death was measured as percentages of DN3 thymocytes from the Lck-Cre^{+} *Cxcr4*$^{+/+}$ and Lck-Cre^{+} *Cxcr4*$^{fl/fl}$ that become annexin V-positive in OP9-DL1 co-cultures on the indicated days (*n*=2). (**b**) Representative histogram showing profile of annexin V staining of cells described in **a** on day 2 and day 6 (*n*=2). (**c**) *Bcl2a1* mRNA expression in DN3e, DN3L and DN4 thymocytes sorted from Lck-Cre^{+} *Cxcr4*$^{+/+}$ and Lck-Cre^{+} *Cxcr4*$^{fl/fl}$ mice was measured by quantitative PCR. Expression was normalized to *Gapdh*, and the DN3e population from Lck-Cre^{+} *Cxcr4*$^{+/+}$ mice was set as the arbitrary unit of 1 to allow relative quantification (*n*>3). (**d**) *Bcl2a1* mRNA expression was tested by quantitative PCR in purified DN cells from PBS or anti-CD3 treated Lck-Cre^{+} *Cxcr4*$^{+/+}$ and Lck-Cre^{+} *Cxcr4*$^{fl/fl}$ mice. The saline-injected population from Lck-Cre^{+} *Cxcr4*$^{+/+}$ mice was set as the arbitrary unit of 1 to allow relative quantification (*n*=2).

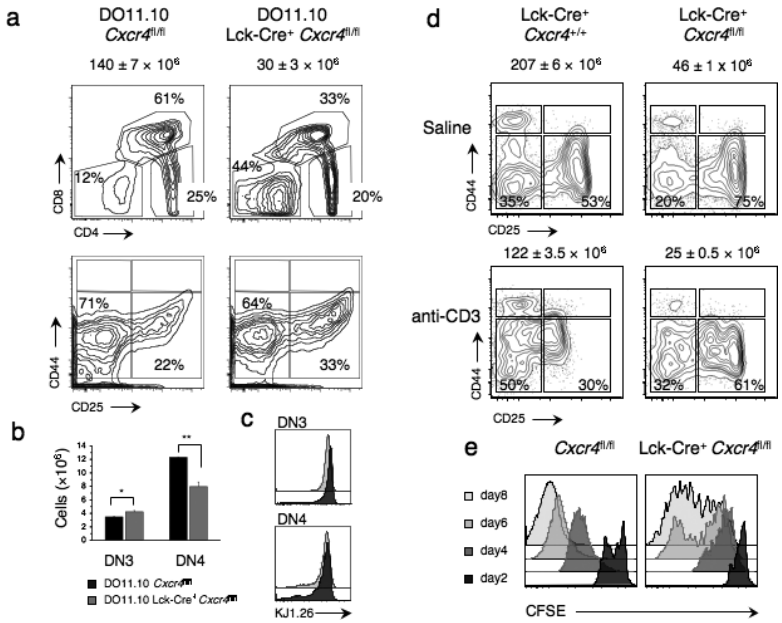

Figure 5. CXCR4 acts a costimulator for the pre-TCR

(**a**) Thymi from Lck-Cre^{+} *Cxcr4*$^{+/+}$ and Lck-Cre^{+} *Cxcr4*$^{fl/fl}$ mice expressing the DO11.1 TCR transgene were isolated. Absolute thymocyte numbers were quantified and surface marker expression was assessed by flow cytometry. Top dot plots were gated on total thymocytes and bottom dot plots on DN cells (*n*=3). (**b**) Absolute numbers of DN3 and DN4 thymocytes in mice analyzed in **a** were calculated by multiplying total thymocyte numbers by the percent distribution of different thymic subsets. Data were plotted as the mean ± s.d. of 4-6 week old littermates for each genotype, obtained from three or more different breeding cages. (**c**) DO11.10 TCR surface expression on the indicated thymocyte subsets was determined using the clonotypic KJ126 antibody. (**d**) Lck-Cre^{+} *Cxcr4*$^{+/+}$ and Lck-Cre^{+} *Cxcr4*$^{fl/fl}$ mice were intraperitoneally injected with saline or anti-CD3. Forty-eight hours later, thymi were collected, single cell suspensions were counted and stained for the indicated differentiation markers. Dot plots are gated on DN thymocytes (*n*=2). (**e**) To assess cell proliferation, DN thymocytes from Lck-Cre^{+} *Cxcr4*$^{+/+}$ and Lck-Cre^{+} *Cxcr4*$^{fl/fl}$ mice were labeled with CFSE and cultured with OP9-DL1 stromal cells. CFSE dilution was measured at the indicated time points by flow cytometry. (*n*=2).

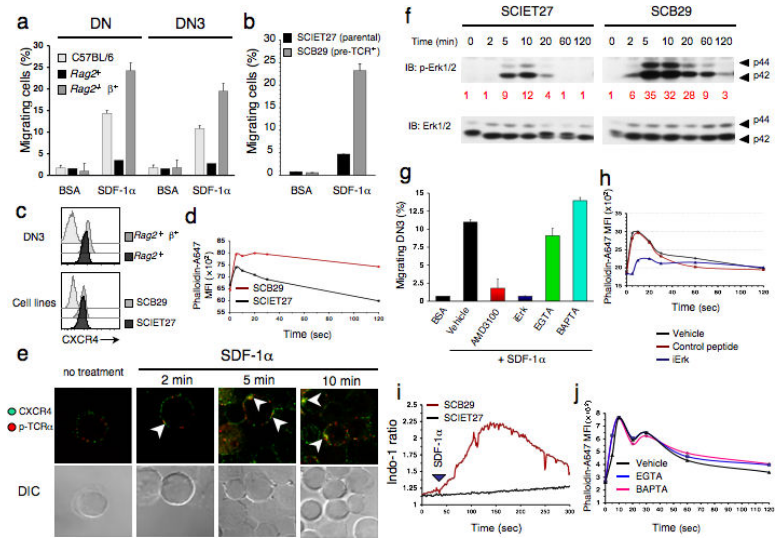

Figure 6.

The pre-TCR regulates CXCR4 signaling and physically associates with CXCR4. (**a**) Purified DN thymocytes from C57BL/6, *Rag2*$^{-/-}$ and *Rag2*$^{-/-}$ TCRβ^{+} mice were tested for chemotaxis to 10nM SDF-1α or bovine serum albumin (BSA) (*n*=5). (**b**) Migration of pre-T cell lines SCIET27 (pre-TCR-deficient) and SCB29 (pre-TCR-expressing) to 20nM SDF-1α or BSA (*n*=5). Data in **a** and **b** are presented as the percentage of input cells that migrate to SDF-1α. (**c**) CXCR4 surface expression on thymocytes from *Rag2*$^{-/-}$ and *Rag2*$^{-/-}$TCRβ^{+} mice and SCIET27 and SCB29 cells was measured by flow cytometry. Light grey histograms indicate isotype control antibody (*n*=3). (**d**) SCIET27 and SCB29 cells were stimulated for the indicated time periods with SDF-1α. F-actin polymerization was analyzed by flow cytometry using Alexa-647-labeled phalloidin. Data show MFI of phalloidin staining. *n*=2. (**e**) SCB29 cells were stimulated for the indicated time periods with SDF-1α, and staining for CXCR4 (green) and pre-TCR (red) was analyzed by confocal microscopy. The images shown are representative of multiple cells on the same slide with similar phenotype (*n*=2). White arrowheads denote close interaction between pre-TCR and CXCR4. (**f**) SCIET27 and SCB29 cells were stimulated for the indicated times with SDF-1α and Erk phosphorylation was measured by immunoblotting. Red numbers indicate densitometry analysis of Erk phosphorylation normalized to total Erk expression. (*n*=5). (**g**) DN3 thymocytes from C57BL/6 mice were treated with a membrane-permeable Erk inhibitory peptide (iErk), the CXCR4 antagonist AMD3100 or the calcium chelators EGTA and BAPTA. Migration to SDF-1α was then assessed using Transwells. Bar graphs show percentage of migrated DN3 cells as a fraction of total cell input, ± s.d. (*n*=2). (**h**) DN3 thymocytes pre-treated with iErk or a control Flag peptide or vehicle alone, and were stimulated with SDF-1α. F-actin polymerization was assessed by flow cytometry. (*n*=2). (**i**) SCIET27 and SCB29 cell lines were stimulated with SDF-1α and calcium flux was measured by spectrofluorimetry (*n*=2). (**j**) SCB29 cells were left untreated or were treated with the calcium chelators EGTA or BAPTA. F-actin polymerization after SDF-1α stimulation was assessed by flow cytometry. (*n*>2).

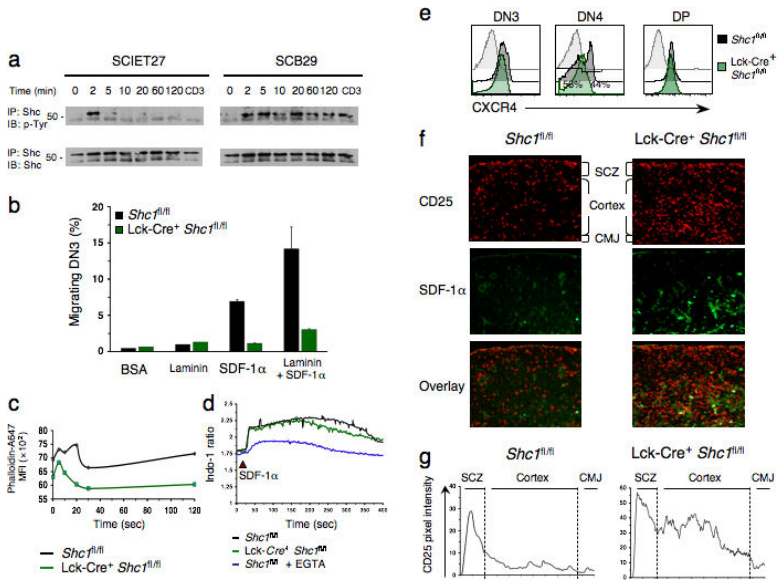

Figure 7.

ShcA is an essential player downstream of CXCR4 signaling for migration and localization of DN thymocytes. (**a**) SCIET27 and SCB29 cells were stimulated for the indicated times with SDF-1α, or with anti-CD3 (positive control). Tyrosine phosphorylation of SchA was assessed by immunoblotting. (*n*=3). (**b**) Thymocytes from *Shc1*$^{fl/fl}$ and *Lck*-Cre+*Shc1*$^{fl/fl}$ mice (four mice for each group) were stimulated or not with SDF-1α, and chemotaxis through laminin or BSA-coated cells was measured. Graphs show the percentage of migrated DN3 cells compared to input. (*n*=4). (**c**) Thymocytes from indicated mice were stimulated with SDF-1α, and F-actin polymerization was measured at the indicated time points. (*n*=2). (**d**) Purified indo-1 labeled DN thymocytes were stimulated with SDF1-α and calcium flux was measured using a fluorimeter. Where indicated, thymocytes were pre-incubated with EGTA. (*n*=2). (**e**) CXCR4 expression on the surface of thymocyte subsets was measured by flow cytometry. Light gray histogram indicates isotype control antibody staining. DP thymocytes from the Lck-Cre^{+} *Shc1*$^{fl/fl}$ mice served as a control since these represent ‘normal’ thymocytes that escaped Cre-mediated deletion43. (*n*>3). (**f**) Thymic cryosections from *Shc1*$^{fl/fl}$ and Lck-Cre^{+} *Shc1*$^{fl/fl}$ littermates were stained for CD25 (red) and SDF-1α (green). Original magnification ×10. (*n*=6). (**g**) Average CD25 pixel intensities derived from scanning serial sections shown in **f** (three mice per each group).